

# Robustness and stability of half-metallic ferromagnetism in alkaline-earth metal mononitrides against doping and deformation

K. Özdoğan\*

*Department of Physics, Yıldız Technical University, 34210 İstanbul, Turkey*

E. Şaşoğlu†

*Peter Grünberg Institut and Institute for Advanced Simulation,  
Forschungszentrum Jülich and JARA, 52425 Jülich, Germany  
and Department of Physics, Fatih University, 34500, Büyükcçekmece, İstanbul, Turkey*

I. Galanakis‡

*Department of Materials Science, School of Natural Sciences, University of Patras, GR-26504 Patra, Greece*

We employ ab-initio electronic structure calculations and study the magnetic properties of CaN and SrN compounds crystallizing in the rocksalt structure. These alkaline-earth metal mononitrides are found to be half-metallic with a total spin magnetic moment per formula unit of  $1.0 \mu_B$ . The Curie temperature is estimated to be 480 K for CaN and 415 K for SrN well-above the room temperature. Upon small degrees of doping with holes or electrons, the rigid-band model suggests that the magnetic properties are little affected. Finally we studied for these alloys the effect of deformation taking into account tetragonalization keeping constant the unit cell volume which models the growth on various substrates. Even large degrees of deformation only marginally affect the electronic and magnetic properties of CaN and SrN in the rocksalt structure. Finally, we show that this stands also for the zincblende structure. Our results suggest that alkaline-earth metal mononitrides are promising materials for magnetoelectronic applications.

PACS numbers: 75.50.Cc, 75.30.Et, 71.15.Mb

## I. INTRODUCTION

Half-metallic ferromagnetic or ferrimagnetic materials have been extensively studied during the last decade due to their potential application in magnetoelectronic devices.<sup>1-3</sup> These magnetic systems present a usual metallic behavior concerning their majority-spin electrons and a semiconducting gap in the minority-spin electronic band structure and thus 100% spin-polarization at the Fermi level and could in principle maximize the efficiency of spintronic devices.<sup>4</sup> As expected the main interest has been focused in the potential half-metallic magnets based on transition-metal elements but the latter due to their large spin-magnetic moments are expected to present large external stray magnetic fields and thus devices based on them should exhibit considerable energy losses. A way to detour this problem is to search for new materials presenting much smaller spin magnetic moments and to this respect a very interesting case are ferromagnetic compounds which do not contain transition-metal atoms. These are widely known in literature with various names like  $d^0$  magnets,  $p$ -ferromagnets or  $sp$ -electron ferromagnets.<sup>5</sup> Several of them combine ferromagnetism with the desired for applications half-metallicity.

There are several ways to create  $sp$ -electron ferromagnets and an extensive review is given in Ref. 5. First, we can induce vacancies or holes at the cation sites in oxides, which lead to a small exchange-splitting of the cation spin-up and spin-down states and thus to half-metallic ferromagnetism.<sup>5-10</sup> A second route to  $p$ -

magnets are the so-called molecular solids.<sup>5</sup> In these materials the oxygen or nitrogen atoms form dimers which are ferromagnetically or antiferromagnetically coupled between them.<sup>11-16</sup> The third way to create half-metallic  $sp$ -electron ferromagnets is the doping of oxides with nitrogen atoms.<sup>5</sup> N impurities at anionic sites (oxygen) present a splitting of their  $p$ -bands and the majority-spin states are completely occupied while the minority-spin states are partially occupied leading to half-metallicity.<sup>17-22</sup> Experimental evidence for the occurrence of magnetism in N-doped MgO has been provided by Liu and collaborators.<sup>23</sup>

An alternative way to half-metallic  $sp$ -electron ferromagnets is the growth of I/II-IV/V nanostructures in metastable lattice structures similar to the case of transition-metal pnictides and chalcogenides in the metastable zincblende structure.<sup>24</sup> Several studies to this research direction have appeared following the pioneering papers published by Geshi et al<sup>25</sup> and Kusakabe et al<sup>26</sup> who have shown using first-principles calculations that CaP, CaAs and CaSb alloys present half-metallic ferromagnetism when grown in the zincblende structure. Ca atom provides two valence electrons (occupying the 4s states in the free atom) while the anions (P,As,Sb) provide 5 valence electrons (*e.g.* in free atom of As the atomic configuration is  $4s^2 4p^3$ ). In total there are 7 valence electrons per unit cell. The first two occupy the  $s$ -valence states created by As atoms which lie deep in energy. The  $p$ -states of anions hybridize strongly with the triple-degenerated  $t_{2g}$   $d$ -states of Ca, which transform following the same symmetry operations, and form

bonding and antibonding hybrids which are separated by large energy gaps. The bonding hybrids contain mostly p-admixture while the antibonding hybrids are mainly of d-character. The remaining 5 valence electron occupy the bonding hybrids which are mainly of anionic p-character in such a way that all three majority-spin p-states are occupied while in the minority-spin band the Fermi level cross the bands so that only the two out of three p-states are occupied. This gives in total a spin magnetic moment per formula unit of exactly  $1 \mu_B$ . This mechanism is similar for all half-metallic ferromagnetic I/II-IV/V alloys in all three zincblende (ZB), wurtzite (WZ) and rocksalt (RS) metastable structures, and the spin magnetic moment follows a Slater-Pauling behavior with the total spin magnetic per formula unit in  $\mu_B$  being 8 minus the number of valence electron in the unit cell:  $M_t = 8 - Z_t$ . Evidence of the growth of such nanostructures has been provided by Liu et al who have reported successful self-assembly growth of ultrathin CaN in the rocksalt structure on top of Cu(001).<sup>27</sup> Finally we have to note that materials containing C or N seem to be more promising for applications since the Hund energy for the light atoms in the second row of the periodic table is similar to the Hund energy of the 3d transition metal atoms.

Following the Refs. 25 and 26 mentioned in the previous paragraph a lot of studies on such compounds have appeared based on first principles calculations and we will give a short overview of them. Although extensive studies exist also for the alkali metal alloys<sup>28-33</sup> and the alkaline earth chalcogenides,<sup>34-40</sup> most of the attention has been focused on the alkaline-earth metal (IInd column) compounds with the Vth-column elements and mainly the nitrides.<sup>25,26,28,41-48</sup> Sieberer et al studied all possible II-V combinations in the ZB and WZ structures and found that all alloys containing Ca, Sr and Ba are half-metallic while only MgN was half-metallic between the Mg-based compounds.<sup>28</sup> It was also shown in Ref. 28 that the ferromagnetic state is energetically preferable to both the non-magnetic and the antiferromagnetic configurations. Volnianska and Boguslawski, as well as Geshi and collaborators have studied the alkaline-earth metal nitrides and have shown that the RS is the more stable structure with formation energies of about -11 eV per unit cell.<sup>43,44</sup> Gao et al have shown that among the RS alloys containing Ca, Sr or Ba as a cation and N, P or As as an anion only the nitrides are stable half-metallic ferromagnets with a total spin magnetic moment of  $1 \mu_B$  and cohesive energies about -9 eV per formula unit.<sup>45</sup> Droghetti and collaborators have shown that RS-MgN is in verge of the half-metallicity and suggested that MgN inclusion upon the N-doping of MgO should lead to a material suitable for magnetic tunnel junctions.<sup>46</sup> The most recent studies on nitrides concern the Curie temperature in the ZB-structure which was found to be 430 K in CaN,<sup>47</sup> and the RS-CaN/ZB-InN and RS-SrN/ZB-GaP (111) interfaces which were found to retain half-metallicity only when the interface is made up from Ca-N or N-In atoms in the first case and N-Ga in the second case.<sup>48</sup>

## II. MOTIVATION AND COMPUTATION METHOD

As we can conclude from the discussion in the previous section, rocksalt alkaline-earth metal nitrides combine some unique properties among these alloys : they have a small spin magnetic moment per formula unit ( $1 \mu_B$ ) and thus create small external magnetic fields, (ii) they present very stable half-metallicity upon hydrostatic pressure, (iii) their equilibrium lattice constant are close to a lot of semiconductors, (iv) results on the ZB-structure suggest high values of the Curie temperature also for the RS-structure, (v) the half-metallic gaps are wide, and (vi) interfaces with semiconductors retain half-metallicity. Thus in this manuscript we complete the previous studies on the RS CaN and SrN alloys focusing on properties which have not yet been determined. In the first part of our study we employ the augmented spherical waves method (ASW)<sup>49</sup> within the atomic-sphere approximation (ASA)<sup>50</sup> in conjunction to the generalized gradient approximation (GGA) for the exchange-correlation potential<sup>51</sup> to perform ground state electronic structure calculations for RS CaN and SrN using the lattice constants from Ref. 44 (5.02 Å for CaN and 5.37 Å for SrN). Notice that within ASW, empty spheres have been used, where needed, in order to describe better the lattice filling. We use these results and the frozen-magnon technique<sup>52</sup> to determine the exchange constants and Curie temperature in both the mean-field (MFA) and random-phase (RPA) approximations. The formalism has been already presented for a one-sublattice system like the ones under study (only N-N interactions contribute since the Ca(Sr) atoms have negligible spin magnetic moments) in Ref. 53. Then using a rigid band model as in Ref. 54 we study how the exchange constants, Curie temperature, spin-polarization and spin magnetic moments vary with the band-filling. In the second part of our study we employ the full-potential nonorthogonal local-orbital minimum-basis band structure scheme (FPLO)<sup>55</sup> within the GGA approximation<sup>51</sup> to determine the equilibrium lattice constants of rocksalt CaN and SrN which are found to be almost identical to the results of Geshi et al.<sup>44</sup> We, thereafter, study the effect on the electronic and magnetic properties of tetragonalization keeping the volume of the unit cell constant which usually accounts for growth on different substrates. To make this study more complete we compare these results with the results also on the zincblende lattice structure.

## III. ROBUSTNESS OF CURIE TEMPERATURE AGAINST DOPING

We will start the presentation of our results from the temperature related properties. As discussed above we employed the ASW method to study the electronic properties of both CaN and SrN in the rocksalt structure using as lattice parameters the equilibrium ones from Ref.

TABLE I: Calculated magnetic properties for the CaN and SrN alloys in the rocksalt structure using the ASW method. The spin magnetic moments are given in  $\mu_B$  units and the Curie temperatures in Kelvin. The lattice constants are the ones determined in Ref. 44.

	$a(\text{\AA})$	$m^{\text{Ca(Sr)}}$	$m^{\text{N}}$	$m^{\text{Total}}$	$T_C^{\text{MFA}}$	$T_C^{\text{RPA}}$
CaN	5.02	0.015	0.980	1.00	620	480
SrN	5.37	0.007	0.995	1.00	594	418

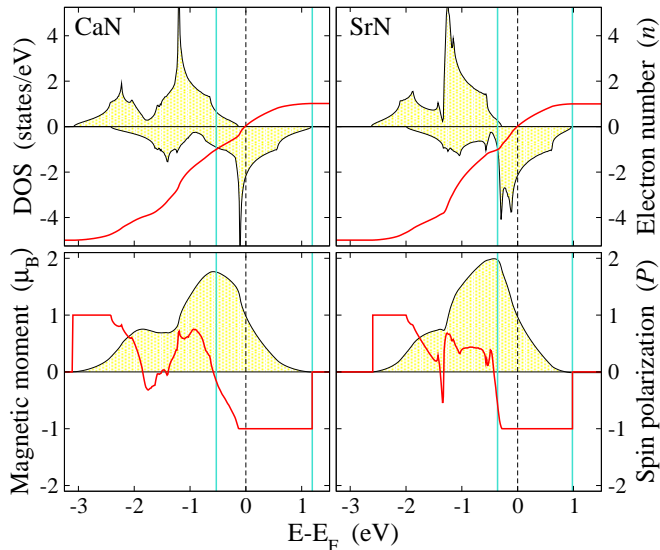


FIG. 1: (Color online) Upper panel: Total DOS (shaded region) for both CaN and SrN alloys in the rocksalt structure using the ASW method. The red line represents the electron counting setting as zero the electrons at the Fermi level. With cyan vertical solid lines we denote the cases of  $\pm 1$  electron. Lower panel: total magnetic moment (shaded region) and spin-polarization (red line) as a function of the electron counting.

44. In Table I we have gathered the calculated magnetic properties. The spin magnetic moments present similar behavior as in the studies discussed in Section I. Both compounds present a total spin magnetic moment per formula unit of  $1 \mu_B$  in agreement with the Slater-Pauling rule for half-metallic mononitrides (there are in total 7 valence electron per unit cell) and thus we expect the density of state (DOS) to present half-metallic properties. Almost all the moment is concentrated at the N atoms. Ca atom carries a spin magnetic moment of only  $0.015 \mu_B$  and Sr of  $0.007 \mu_B$ . Thus the cation-cation as well as the cation-nitrogen interactions should make a minimal contribution to the exchange constants and it is enough to consider the N-N intrasublattice magnetic interaction when discussing the temperature related properties. The very small spin magnetic moments at the cationic site reflect the very small charge at these sites since the occupied bonding hybrids are mainly of anionic character having only a very small cationic d-admixture as discussed in Section I.

The total DOS for both compounds are presented in Fig. 1. We do not present the deep-lying occupied s-states since they are located at about  $-12$  eV below the Fermi level and thus are not relevant for the discussion of the electronic properties. The bonding and the antibonding hybrids are separated by a gap which is about  $1.7$  eV for the minority-spin states; the antibonding hybrids are not presented in the figure. Note also that the antibonding states present almost no exchange splitting. Ca(Sr)-resolved DOS is very small with respect to the N-resolved DOS in the energy window, of the occupied states and thus we can safely assume that the total DOS presented in the figure coincides in this energy window with the N-resolved DOS. The Fermi level cross the minority-spin DOS while all the majority N p-states are occupied and the Fermi level falls within a majority-spin gap which is  $3.1$  eV wide for CaN and  $3.0$  for SrN. The so-called half-metallic gap, defined as the energy distance between the highest occupied majority-spin state and the Fermi level, is about  $0.1$  eV for CaN and  $0.2$  eV for SrN.

Small degrees of doping can be assumed to result in small shifts of the Fermi level as assumed also for the semi-Heusler compounds in Ref. 54. In Fig. 1 we present in the upper panel the total DOS for both CaN and SrN alloys and with the red line the electron counting setting the number of electrons at the Fermi level as zero. The vertical blue lines denote the limits of  $\pm 1$  electron. As we dope our system with electrons and we move to higher values of the energy with respect to the Fermi level we populate also the minority-spin bonding hybrids. For exactly a surplus of one electron per formula unit all minority-spin bonding hybrids are occupied (we remind here that in these alloys two out of three minority-spin p-states were already occupied) and we end up with a compound with zero total spin magnetic moment. This situation is probably unphysical since it corresponds to a very large degree of doping and ScN and YN in the rocksalt structure which have one more valence electron than CaN and SrN are semiconductors. If we start doping CaN and SrN with holes we move deeper in energy. The two alloys present a significant difference in their behavior due to the larger exchange-splitting in the case of SrN which is also reflected on the larger half-metallic gap. As shown by the spin-polarization presented with the red line in the lower panel of Fig. 1, for CaN small doping with holes results very quickly in loss of half-metallicity and the spin polarization deviates from the perfect 100%. On the other hand in SrN even doping with one hole preserves the half-metallic character and the perfect spin-polarization since the Fermi level is at the verge of the occupied majority-spin electronic bands. In the lower panel of the same figure we also present the variation of the spin-magnetic moment with the electron counting which also reflects our discussion. Exactly at the Fermi level we have a total spin magnetic moment of  $1 \mu_B$  and when we dope with holes it increases. For one hole (corresponding to  $-1$  electron in the counting) the spin magnetic moment of CaN reaches a value of  $1.76 \mu_B$

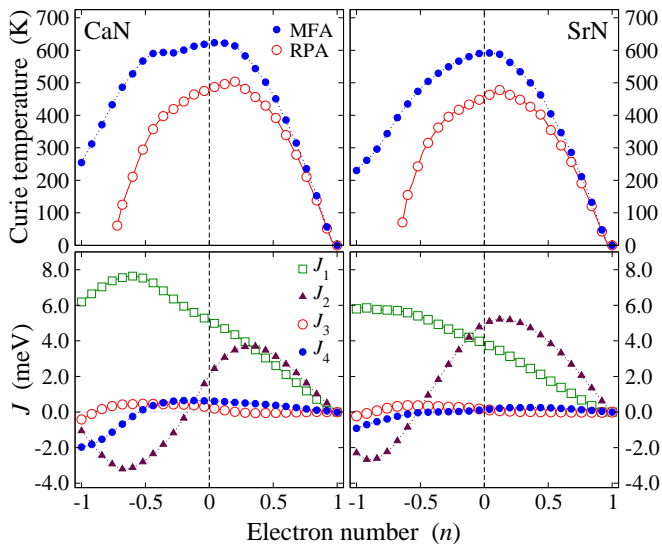


FIG. 2: (Color online) Upper panel: Calculated Curie temperatures within both the random-field (RPA) and mean-field (MFA) approximations for CaN and SrN in the rocksalt structures as a function of the electron counting (see Fig. 2). Lower panel: Calculated exchange constants between nitrogen atoms as a function of the electron counting up to fourth neighbors. The N-Ca(Sr) and Ca(Sr)-Ca(Sr) exchange constants are negligible with respect to the N-N ones due to the very small spin magnetic moment of the Ca(Sr) atoms.

while for SrN the hole populates only minority-spin states and the spin moment reaches the value of  $2 \mu_B$  expected from the Slater-Pauling rule for perfect half-metals. Of course doping with electrons leads to a decrease of the total spin magnetic moment which vanishes when we add exactly one electron to our system and all bonding hybrids are occupied.

In the last part of this section we will concentrate on the Curie temperatures. In Table I we present the estimated values of the Curie temperature in Kelvin. The mean field approximation (MFA) gave a value of 620 K for CaN and 594 K for SrN while the random-phase approximation (RPA) gave values of 480 K and 418 for CaN and SrN, respectively. RPA is expected to give more accurate results with respect to MFA since RPA corresponds to a larger weight of the lower-energy excitations contrary to MFA which assumes an equal weight for both low- and high-energy excitations.<sup>53</sup> The calculated Curie temperatures exceed significantly the room temperature as was also the case for various sp-electron ferromagnets discussed in Section I and thus these alloys can have potential room-temperature applications in spintronic devices. Note that for CaN in the zincblende structure we had calculated within RPA in Ref. 47 a value for the Curie temperature of 415 K which is lower than the 480 K for the rocksalt-CaN in the present study although the nitrogen atoms have a spin magnetic moment of  $0.98 \mu_B$  in both ZB and RS structures.

In Fig. 2 we present how the calculated Curie tem-

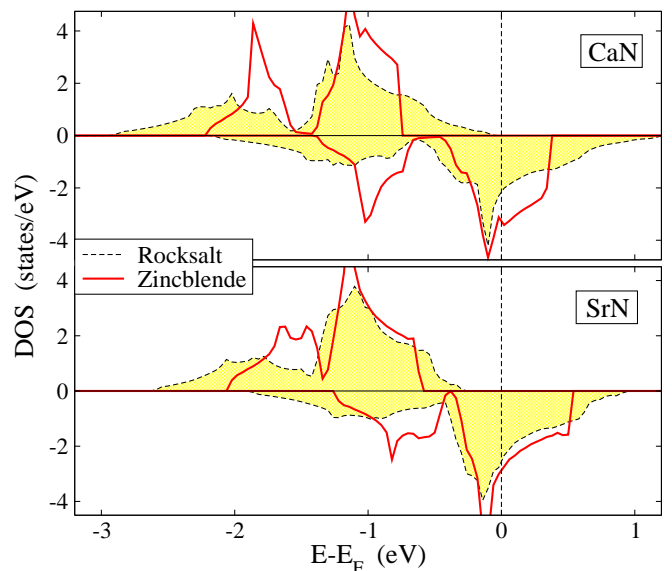


FIG. 3: (Color online) Total DOS of CaN and SrN alloys in both the rocksalt (shaded region) and zincblende (red thick lines) structures using the FPLO method. Calculations are performed at the calculated GGA equilibrium lattice constants ( $5.02 \text{ \AA}$  and  $5.45 \text{ \AA}$  for CaN in the rocksalt and zincblende structures, respectively, and  $5.39 \text{ \AA}$  and  $5.82 \text{ \AA}$  for SrN in the same two lattice structures respectively). Details as in Fig. 1.

perature and the exchange constants in the N-sublattice behave with respect to the electron counting. We focus in a window of  $\pm 1$  electron although usual doping with electrons or holes should result to a much smaller change in the electronic counting. In all cases MFA results are higher than the RPA ones and as we move to the case +1 electron the MFA and RPA values coincide. At the vicinity of the zero electron counting the estimated Curie temperature still exceeds considerably the estimated room temperature. For both CaN and SrN the calculated RPA temperature reaches the room temperature either for doping with 0.6 electrons or for doping with 0.5 holes and thus for moderate degrees of doping we are well above the room temperature. At the zero of the electron counting we get the maximum Curie temperature due to the combination of the contribution of the exchange constants between both N-N nearest ( $J_1$ ) and next-nearest ( $J_2$ ) neighbors as shown in the lower panel of Fig. 2. Exactly at zero electron counting both  $J_1$  and  $J_2$  favor ferromagnetism and make important contribution to the Curie temperature. In SrN with respect to CaN the  $J_2$  takes larger values while the opposite occurs for  $J_1$ . As we dope with electrons  $J_1$  starts dropping fast, while when we dope with holes  $J_1$  increases considerably but at the same time  $J_2$  starts favoring antiferromagnetism leading also to smaller estimated Curie temperatures. The interaction between N-N third and fourth neighbors are significant only at the vicinity of the -1 electron value for the electron counting.



TABLE II: Calculated spin magnetic moments (in  $\mu_B$ ) for SrN in both rocksalt and zincblende structure using the FPLO method within the GGA approximation. The first line corresponds to the ideal equilibrium lattice constants and the rest to tetragonalization where we vary the in-plane lattice parameters by the percentage shown in the second column and in the same time we vary also the lattice parameter along the c-axis so that the unit-cell volume is kept equal to the equilibrium one. Note that in the second column the minus "-" sign means compression and the plus "+" sign means expansion. In all cases the total spin-magnetic is kept equal to  $1.0 \mu_B$  and thus the half-metallicity is preserved. Similar are the results for CaN, where the only noticeable difference is that in all cases the absolute values of Ca and N spin moments are smaller by about  $0.01\mu_B$  with respect to SrN and thus they sum up again to  $1.0 \mu_B$ .

	Case	SrN-RockSalt (5.39Å)			SrN-ZincBlende (5.82Å)		
		Sr	N	Total	Sr	N	Total
Ideal		-0.074	1.074	1.000	-0.093	1.093	1.000
Tetragonalization	-1%	-0.074	1.074	1.000	-0.093	1.093	1.000
	-5%	-0.073	1.073	1.000	-0.093	1.093	1.000
	-10%	-0.068	1.068	1.000	-0.093	1.093	1.000
	+1%	-0.074	1.074	1.000	-0.093	1.093	1.000
	+5%	-0.072	1.072	1.000	-0.093	1.093	1.000
	+10%	-0.069	1.069	1.000	-0.094	1.094	1.000

#### IV. STABILITY OF HALF-METALLICITY AGAINST LATTICE DEFORMATION

In the second part of our study we will focus on the stability of half-metallicity against lattice deformations. To carry out these calculations as stated in Section II we have employed the FPLO<sup>55</sup> code, which is a full potential code and thus is expected to describe tetragonal deformations more accurately than the ASW<sup>49</sup> code which employs the atomic sphere approximation.<sup>50</sup> Since we are interested in deformations the first step is to calculate the equilibrium lattice constants using total energy calculations. To this respect we have employed the GGA approximation which is well-known to produce more accurately results concerning the elastic properties than the local-spin density approximation (LSDA). For CaN in the rocksalt structure we found an equilibrium lattice constant of 5.02 Å and for SrN 5.39 Å. These values are almost identical to the results of Geshi and collaborators who found for rocksalt CaN and SrN 5.02 Å and 5.37 Å, respectively. To make our study on deformations more complete we have also included the case of zincblende CaN and SrN since the tetragonalization effect has not yet been studied for this structure. Our FPLO-GGA total energy calculations gave as an equilibrium lattice constant of 5.45 Å for CaN and 5.82 Å for SrN in the ZB-lattice. The lattice constant of the ZB cubic unit cell is larger than in the RS-structure since in the former case it also contains two void sites while no voids are present in the RS-case. In Fig. 3 we present the total DOS for both compounds and for both ZB and RS lattices at the equilibrium lattice constants. In the RS-case our DOS within FPLO are similar to the ASW DOS in Fig. 1. In the ZB-cases the bands are more narrow than the RS-structure and again both CaN and SrN are half-metallic ferromagnets with a total spin magnetic in the formula unit of  $1 \mu_B$ . For the ZB-lattice the half-metallic gaps are considerable larger being around 0.5 eV for SrN and slightly larger for CaN.

To simulate deformation of the lattices with respect to equilibrium we took into account the case of tetragonalization where we vary both the in-plane and out-of-plane parameters keeping the unit cell volume constant to the equilibrium. Such a deformation is expected to model the growth of the materials under study on different substrates. In Table II we have gathered our results concerning the spin magnetic moments for SrN in both RS- and ZB-lattices. We do not present the results for CaN since the effect of deformation is identical for both alloys although their electronic band structure in Fig. 3 present slight differences. In the second column we present the percentage of change; "-" means compression by that percentage and "+" means expansion, and the percentage refers to the in-plane lattice constants. We took six values of the percentage into account:  $\pm 1\%$ ,  $\pm 5\%$  and  $\pm 10\%$ . In all cases the SrN compound remains half-metallic in both the RS and ZB structures with a total spin magnetic moment of  $1 \mu_B$ . Deformations lead to small changes of the absolute values of the Sr and N atomic spin magnetic moments of less than  $0.01 \mu_B$  in such a way that they cancel each other keeping the total spin moment constant. Even in the case of CaN (not presented here) in the RS structure where the half-metallic gap is only 0.1 eV (see discussion in Section III) the half metallic character is preserved even for a  $\pm 10$  deformation. Our calculated DOS (note presented) confirm the conclusion drawn from the spin magnetic moments and are identical to the ideal cubic lattice for all degrees of tetragonalization under study.

Finally we should also shortly comment on the expected behavior of the Curie temperature upon tetragonalization. In Refs 56 and 57 it was shown by means of first-principles calculations that the Curie temperature in Heusler compounds increases with increasing hydrostatic pressure which is in agreement with the initial Castellan interaction curve based on experiments for transition metal compounds<sup>58</sup> and its recent generalization for Heusler alloys by Kanomata and collaborators.<sup>59</sup> For the

sp-electron ferromagnets under study we expect a similar behavior since in Ref. 47 we have shown that the Curie temperature is very sensitive to the lattice spacing in zincblende pnictides and this also led to the larger Curie temperature for CaN with respect to SrN (the former has smaller lattice parameter). Tetragonalization keeping the volume constant is not expected to change the Curie temperature. If, e.g., we have smaller exchange parameters within the  $xy$ -plane with respect to the equilibrium due to expansion, the compression in the out of-plane  $z$ -axis will lead to larger exchange constants, eventually compensating each other. Only in cases where strain induces volume changes, like in the case of hydrostatic pressure or tetragonalization keeping the in-plane lattice parameters constant, one could expect variation in the estimated Curie temperatures.

## V. SUMMARY AND CONCLUSIONS

Half-metallic ferromagnets, which do not contain transition metal atoms, are attractive for applications due to the smaller spin magnetic moments. Among these so-called sp-electron ferromagnets the case of alkaline-earth metal mononitrides crystallizing in the rocksalt, wurtzite or zincblende structures are promising since the half-metallicity is combined with a total spin-magnetic moment of  $1 \mu_B$  per formula unit leading to minimal energy losses in spintronic applications. Moreover their equilibrium lattice constant makes them suitable for growth on top of a variety of semiconductors.

In the present study we have concentrated on the rocksalt structure of CaN and SrN which is energetically favored with respect to the wurtzite and zincblende ones. Employing electronic-structure calculations in conjunc-

tion with the generalized gradient approximation and using the frozen-magnon technique we have studied the temperature dependent properties upon varying the electron counting. Both alloys were found to present Curie temperature above the room temperature (480 K for CaN and 415 K for SrN using the random-phase approximation). Upon small degrees of doping either with electrons or holes the Curie temperature presented only a small decrease from its maximum value, and we had to dope it with  $\sim 0.6$  electrons or  $\sim 0.5$  holes per formula unit for the Curie temperature to become comparable to the room temperature. At the zero electron counting (no doping) both the nearest and next-nearest N-N interaction favored ferromagnetism; as we dope with electrons their intensity decrease, while as we dope with holes the nearest N-N exchange interaction becomes more sizeable while the next-nearest N-N interaction starts favoring an antiferromagnetic configuration leading to the decrease of the Curie temperature.

In the second part of our study we studied the response of both the electronic and magnetic properties upon tetragonalization keeping the unit cell volume constant. Except the rocksalt we performed calculations also for the zincblende lattice for both CaN and SrN. In all cases under study the half-metallicity was preserved and both the electronic and magnetic properties only marginally changed. Moreover, since the unit cell volume remains constant, also the Curie temperature is not expected to vary.

Thus we can conclude that these materials are promising for applications since small degrees of doping or large deformations keep intact the half-metallic character and a high value for the Curie temperature and their controlled experimental growth is expected to boost the interest on sp-electron ferromagnets.

- 
- \* Electronic address: kozdogan@yildiz.edu.tr  
† Electronic address: e.sasioglu@fz-juelich.de  
‡ Electronic address: galanakis@upatras.gr
- <sup>1</sup> I. Žutić, J. Fabian, and S. Das Sarma, *Rev. Mod. Phys.* **76**, 323 (2004).
  - <sup>2</sup> C. Felser, G. H. Fecher, and B. Balke, *Angew. Chem. Int. Ed.* **46**, 668 (2007).
  - <sup>3</sup> H. Zabel, *Materials Today* **9**, 42 (2006).
  - <sup>4</sup> M. I. Katsnelson, V. Yu. Irkhin, L. Chioncel, A. I. Lichtenstein, and R. A. de Groot, *Rev. Mod. Phys.* **80**, 315 (2008).
  - <sup>5</sup> O. Volnianska and P. Boguslawski, *J. Phys.:Condens. Matter* **22**, 073202 (2010).
  - <sup>6</sup> W. Zhou, X. Tang, P. Xing, W. Liu, and P. Wu, *Phys. Lett. A* **376**, 203 (2012).
  - <sup>7</sup> T. Uchino and T. Yoko, *Phys. Rev. B* **85**, 012407 (2012).
  - <sup>8</sup> F. Maca, J. Kudrnovský, V. Drchal, and G. Bouzerar, *Appl. Phys. Lett.* **92**, 212503 (2008).
  - <sup>9</sup> Y. L. Zheng, C. M. Zhen, X. Q. Wang, L. Ma, X. L. Li, and D. L. Hou, *Sol. St. Sci.* **13**, 1516 (2011).
  - <sup>10</sup> L. X. Guan, J. G. Tao, C. H. A. Huan, J. L. Kuo, and L. Wang, *J. Appl. Phys.* **108**, 093911 (2010).
  - <sup>11</sup> E. R. Ylvisaker, R. R. P. Singh, and W. E. Pickett, *Phys. Rev. B* **81**, 180405(R) (2010).
  - <sup>12</sup> R. Kovacik and C. Ederer, *Phys. Rev. B* **80**, 140411(R) (2009).
  - <sup>13</sup> M. Kim, B. H. Kim, H. C. Choi, and B. I. Min, *Phys. Rev. B* **81**, 100409(R) (2010).
  - <sup>14</sup> O. Volnianska and P. Boguslawski, *Phys. Rev. B* **77**, 220403(R) (2008).
  - <sup>15</sup> I. Slipukhina, Ph. Mavropoulos, S. Blügel, and M. Ležaić, *Phys. Rev. Lett.* **107**, 137203 (2011).
  - <sup>16</sup> H. Wu, A. Stroppa, S. Sakong, S. Picozzi, M. Scheffler, and P. Kratzer, *Phys. Rev. Lett.* **105**, 267203 (2010).
  - <sup>17</sup> P. Mavropoulos, M. Ležaić, and S. Blügel, *Phys. Rev. B* **80**, 184403 (2009).
  - <sup>18</sup> W.-Z. Xiao, L.-L. Wang, L. Xu, Q. Wan, and A.-L. Pan, *Sol. St. Commun.* **150**, 852 (2010).
  - <sup>19</sup> V. V. Bannikov, I. R. Shein, and A. L. Ivanovskii, *J. Supercond. Nov. Magn.* **24**, 1693 (2011).
  - <sup>20</sup> K. Yang, Y. Dai, and B. Huang, *Appl. Phys. Lett.* **100**, 062409 (2012).

- <sup>21</sup> K. Kenmochi, V. A. Dinh, K. Sato, A. Yanase, and H. Katayama-Yoshida, *J. Phys. Soc. Jpn* **73**, 2952 (2004).
- <sup>22</sup> K. Kenmochi, M. Seike, K. Sato, A. Yanase, and H. Katayama-Yoshida, *Jpn. J. Appl. Phys.* **43**, L934 (2004).
- <sup>23</sup> C. M. Liu, H.-Q. Gu, X. Xiang, Y. Zhang, Y. Jiang, M. Chen, and X.-T. Zu Xiao-Tao, *Chin. Phys. B* **20**, 047505 (2011).
- <sup>24</sup> Ph. Mavropoulos and I. Galanakis, *J. Phys. Condens. Matter* **19**, 315221 (2007).
- <sup>25</sup> M. Geshi, K. Kusakabe, H. Tsukamoto, and N. Suzuki, 2004 Preprint arXiv:cond-mat/0402641 (2004).
- <sup>26</sup> K. Kusakabe, M. Geshi, H. Tsukamoto, and N. Suzuki, *J. Phys.:Condens. Matter* **16**, S5639 (2004).
- <sup>27</sup> X. Liu, B. Lu, T. Iimori, K. Nakatsuji, and F. Komori, *Surf. Sci.* **602**, 1844 (2008).
- <sup>28</sup> M. Sieberer, J. Redinger, S. Khmelevskiy, and P. Mohn, *Phys. Rev. B* **73**, 024404 (2006).
- <sup>29</sup> C.-W. Zhang, *J. Phys. D.: Appl. Phys.* **41**, 085006 (2008).
- <sup>30</sup> K. Zberecki, L. Adamowicz, and M. Wierzbicki, *Phys. St. Solidi (b)* **246**, 2270 (2009).
- <sup>31</sup> E. Yan, *Physica B* **407**, 879 (2012).
- <sup>32</sup> G. Y. Gao, K. L. Yao, Z. L. Liu, Y. Min, J. Zhang, S. W. Fan, and D. H. Zhang, *J. Phys.:Condens. Matter* **21**, 275502 (2009).
- <sup>33</sup> G. Y. Gao, K. L. Yao, M. H. Song, and Z. L. Liu, *J. Magn. Magn. Mater.* **323**, 2652 (2011).
- <sup>34</sup> G. Y. Gao, K. L. Yao, Z. L. Liu, J. L. Jiang, L. H. Yu, and Y. L. Shi, *J. Phys.:Condens. Matter* **19**, 315222 (2007).
- <sup>35</sup> G. Y. Gao, K. L. Yao, E. Şaşıoğlu, L. M. Sandratskii, Z. L. Liu, and J. L. Jiang, *Phys. Rev. B* **75**, 174442 (2007).
- <sup>36</sup> G. Y. Gao and K. L. Yao, *Appl. Phys. Lett.* **91**, 082512 (2007).
- <sup>37</sup> S. Dong and H. Zhao, *Appl. Phys. Lett.* **98**, 182501 (2011).
- <sup>38</sup> C.-W. Zhang, S.-S. Yan, and H. Li, *Phys. St. Solidi (b)* **245**, 201 (2008).
- <sup>39</sup> G. Y. Gao and K.-L. Yao, *J. Appl. Phys.* **106**, 053703 (2009).
- <sup>40</sup> U. P. Verma, Mohini, P. S. Bisht, and P. Jensen, *Semicond. Sci. Technol.* **25**, 105002 (2010).
- <sup>41</sup> K. L. Yao, J. L. Jiang, Z. L. Liu, and G. Y. Gao, *Phys. Lett. A* **359**, 326 (2006).
- <sup>42</sup> Y. Li and J. Yu, *Phys. Rev. B* **78**, 165203 (2008).
- <sup>43</sup> O. Volnianska and P. Boguslawski, *Phys. Rev. B* **75**, 224418 (2007).
- <sup>44</sup> M. Geshi, K. Kusakabe, H. Nagara, and N. Suzuki, *Phys. Rev. B* **76**, 054433 (2007).
- <sup>45</sup> G. Y. Gao, K. L. Yao, Z. L. Liu, J. Zhang, Y. Min, and S. W. Fan, *Phys. Lett. A* **372**, 1512 (2008).
- <sup>46</sup> A. Droghetti, N. Baadji, and S. Sanvito, *Phys. Rev. B* **80**, 235310 (2009).
- <sup>47</sup> A. Laref, E. Şaşıoğlu, and I. Galanakis, *J. Phys.:Condens. Matter* **23**, 296001 (2011).
- <sup>48</sup> G. Y. Gao, K. L. Yao, and N. Li, *J. Phys.:Condens. Matter* **23**, 075501 (2011).
- <sup>49</sup> A. R. Williams, J. Kübler, and C. D. Gelatt, *Phys. Rev. B* **19**, 6094 (1979).
- <sup>50</sup> O. K. Andersen, *Phys. Rev. B* **12**, 3060 (1975).
- <sup>51</sup> J. P. Perdew, K. Burke, and M. Ernzerhof, *Phys. Rev. Lett.* **78**, 1396 (1997).
- <sup>52</sup> L. M. Sandratskii and P. Bruno, *Phys. Rev. B* **66**, 134435 (2002).
- <sup>53</sup> E. Şaşıoğlu, I. Galanakis, L. M. Sandratskii, and P. Bruno, *J. Phys.:Condens. Matter* **17**, 3915 (2005).
- <sup>54</sup> I. Galanakis and E. Şaşıoğlu, *J. Appl. Phys.* **109**, 113912 (2011).
- <sup>55</sup> K. Koepernik and H. Eschrig, *Phys. Rev. B* **59**, 1743 (1999).
- <sup>56</sup> E. Şaşıoğlu, L. M. Sandratskii, and P. Bruno, *Phys. Rev. B* **71**, 214412 (2005).
- <sup>57</sup> S. K. Bose, J. Kudrnovský, V. Drchal, and I. Turek, *Phys. Rev. B* **84**, 174422 (2011).
- <sup>58</sup> L. Castelliz, *A. Metallkde.* **46**, 198 (1955).
- <sup>59</sup> T. Kanomata, K. Shirakawa, and T. Kaneko, *J. Magn. Magn. Mater.* **65**, 76 (1987).